オンオフ制御によるクラブ・ステアリングの自動操向(1)

誌名	神戸大学農学部研究報告 = The science reports of Faculty of Agriculture, Kobe University
ISSN	04522370
著者	堀尾, 尚志
巻/号	18巻2号
掲載ページ	p. 187-195
発行年月	1989年3月

神大農研報 (Sci. Rept. Fac. Agr. Kobe Univ.) 18 : 187—195, 1989

ON-OFF CONTROL OF CRAB-STEERING (I)
— Stability Analysis —

Hisashi HORIO*

(Received for publication on Angust 10, 1988)

Abstract

Crab-steering is advantageous to be used in the vehicle steering for some kind of field operations, since the zero-yawing steering makes it easy to guide an implement along a desired pass. It may be more abvantageous to be used in automatic steering. In this paper, the response of on-off controlled crab-steering system to harmonic input signal is analyzed using dual-input describing function, and verified by digital simulation.

Introduction

In cultivating operation, the machine is generally steered along the edge of tilled land as a desired pass. This desired pass is nearly straight and has a little lateral offset in some points. As the steering mode of the machine mounting implement is ordinarily front-wheel-steering, the steering operation is done to adjust the position of the implement along the desired pass under taking the influence of changing yaw angle into consideration. Hence the steering-geometrical complexity impedes the automatic steering and the lateral position control of implement was studied as the cooperative control system [1, 2, 3] with usual front-wheel-steering control. If the crab-steering is introduced to steering system, an easy steering operation is realized by zero-yawing characteristics. There are many of similar operations in cultivation, and also in many field operations out of agricultural sector. Although the advantage of crab-steering, it is not widely used in practical machine. As the examples in agricultural machines, the 4WD-tractor presented in the DLG fair in Hanover[4] and the apple harvester manufactured for trial in USA[5] became known. Its practical use may be impeded by its unfamiliar steering mode for common operators.

In the viewpoint of automatic steering, the crab-steering is practically advantageous, since the implement mounted or attached on vehicle at rear or front end moves parallel with the steering direction and also an automatic control system itself is liberal from unfamiliar steering mode. However no research paper on the automatic steering of crab-steering vehicle has been seen through author's survey. The author have studied on the applications of crab-stieering vehicle to automatic tillage[6, 7, 8]. In this paper, the fundamental characteristics of on-off controlled crab-steering system is discussed and analyzed using dual-input describing function. The results of analysis are verified by digital simulation, and discussed.

General Concept of on-off Controlled Crab-Steering System

In on-off controlled steering system, a steering signal is generally detected as three states signal from relative position of sensing unit mounted on vehicle and sensing object upon the ground as desired pass. Two modes

* Agricultural Power and Vehicles,
Department of Agricultural Engineering

of control action in on-off controlled crab-steering system can be considered as follows; traveling direction control (traveling angle control) and lateral position control. In traveling direction control, the steering angle is manipulated to increase or decrease with the steering signals generated by three states relay element, and steering angle is held at the state while tracking error is within dead band. In lateral position control, the steering angle is regulated to be zero when the steering signal becomes off.

In traveling direction control, the feedback variable is the traveling direction detected by the sensing device linked in steering angle. The stability exists in ramp response and does not in step response. In latlral position control, the feedback variable is the lateral displacement detected by sensing device fixed on vehicle body. Stability exists in step response and dose not in ramp response, which has always limit cycles and is like jerking motion.

Steering of field machine in general cultivating operations is done to adjust the implement position for lateral direction. Automatic steering in such operations is regarded as the sequence of step responses. Therefore, lateral position control of vehicle is suitable for field operation traveling of crab-steering vehicle. Although such condition is generally considered, it is also considered that the desired pass has the curve of sinusoidal bent. The analysis on non-autonomous systlm is indispensable.

Describing Function Analysis

In this analysis, the on-off controlled crab-steering system is assumed as follows;

1) On-off signal for steering is generated by three states relay with hysteresis.
2) Output of control system is lateral displacement of the vehicle locus and directly fed back.
3) Steering angle is also controlled by on-off control sub-system composed by three states relay of narrow dead band and the steering mechanism composed from solenoid valve and hydraulic cylinder.
4) The maximum steering angle (MSA) and steering angle velocity are system parameters.

The block diagram of control system is shown in Fig. 1. The output from the relay is transformed in voltage reference to the desired voltage which is corresponding to the settled MSA. The desired voltage and the voltage as a real steering angle fed back through differential transformer are differentially applied on the three states relay with narrow dead band. The solenoid valve is exited by the output signal from the relay and the hydraulic cylinder actuates the drag link arm of axle unit to steer wheels.

There are two nonlinear elements in the block diagram shown in Fig. 1. For simplification the subsystem part for the steering angle control and the final control element are approximated to linear system. This linear equalized system can be considered to

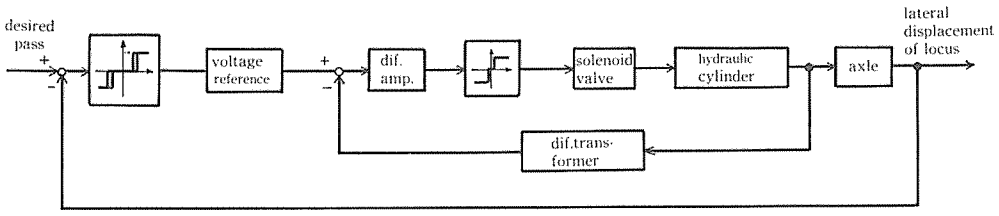

Fig. 1 Block Diagram of Control System

be equivalent for the combination of lag time, integral and second order lag elements as shown in Fig. 2.

The describing function K_{eg} of three states relay with hysteresis is given by[9]

$$K_{eq}=\frac{2M}{\pi E}(\cos\theta_1+\cos\theta_2) -j\frac{2M}{\pi E}(\sin\theta_1-\sin\theta_2) \quad (1)$$

where

$$\cos\theta_1=\sqrt{1-\frac{a_1^2}{E^2}}\ , \quad \sin\theta_1=\frac{a_1}{E},$$

$$\cos\theta_2=\sqrt{1-\frac{a_2^2}{E^2}}\ , \quad \sin\theta_2=\frac{a_2}{E},$$

E is the amplitude of harmonic input to relay, M is the amplitude of output from relay, a_1 and a_2 are thresholds of relay ($2a_1$ is dead band width and a_1-a_2 is hysteresis width).

K_{eq} given by eq. (1) is the equivalent gain in the absence of any external input (autonomous system). Let the input to relay e be

$$e=A\sin(\omega t)+B\sin(\alpha t). \quad (2)$$

It will be assumed that these two harmonic components are independent with each other. The equivalent gain to the input e is given by dual-input describing function $K_{eq}(A, B)$[9, 10]

$$K_{eq}(A, B)=\frac{j}{\pi A}\int_{-\infty}^{\infty}F(ju)J_0(Bu)J_1(Au)du \quad (3)$$

where J_0 and J_1 are respectively zero and first order Bessel functions, and $F(ju)$ is the integral expression of relay characteristics. As x and $r(x)$ are input and output of the relay,

$$F(ju)=\int_{-\infty}^{\infty}r(x)e^{-jux}dx.$$

Here the relay with hysteresis is difficault to be expressed in $F(ju)$, therefore hysteresis is neglected. It is sown[11] that $F(ju)$ for

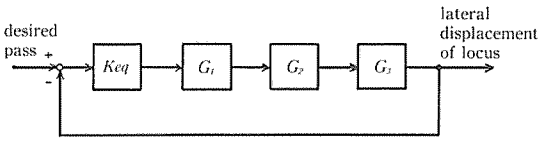

Fig. 2 Linear Equalized Block Diagram of Control System

three states relay is of the form

$$F(ju)=\frac{2M}{j}\cdot\frac{\cos(au)}{u} \quad (4)$$

where a is threshold. Hence dual-input describing function for three states relay is given by

$$K_{eq}(A, B) =\frac{2M}{\pi A}\int_{-\infty}^{\infty}\frac{\cos(au)}{u}J_0(Bu)\ J_1(Au)du\ . \quad (5)$$

The integration in eq.(5) may be expressed as

$$I=2\int_0^{\infty}\frac{\cos(au)}{u}J_0(Bu)\ J_1(Au)du\ . \quad (6)$$

Dividing integral interval by ε $(0<\varepsilon\ll 1)$,

$$I=2\int_0^{\varepsilon}\frac{\cos(au)}{u}J_0(Bu)\ J_1(Au)du +2\int_{\varepsilon}^{\infty}\frac{\cos(au)}{u}J_0(Bu)\ J_1(Au)du \quad (7)$$

then $J_0(Bu)\ J_1(Bu)$ in the intgrand of the first term may be developed to yield

$$J_0(Bu)\ J_1(Au) =\frac{Au}{2}\sum_{n=0}^{\infty}(-1)^n\frac{(Bu/2)^{2n}}{n!\Gamma(n+1)}{}_2F_1\left(-n,\ -n\ ;2\ ;\frac{A^2}{B^2}\right) \quad (8)$$

where Γ is gamma function and ${}_2F_1$ is Gauss' hypergeometric function. Using eq. (8), the integration I_1 in the first term of the right side of eq. (7) may be evaluated to yield

I_1

$$=\frac{A}{2}\sum_{n=0}^{\infty}(-1)\frac{(B/2)^{2n}}{n!\Gamma(n+1)}{}_2F_1(-n,\ -n\ ;2\ ;\frac{A^2}{B^2})$$
$$\times\int_0^{\varepsilon}u^{2n}\cos a\,u\,du\ . \tag{9}$$

The second term in the right side of eq. (7) can be directly evaluated, using computer.

Transfer functions $G_1(s)$, $G_2(s)$ and $G_3(s)$ are given by

$$G_1(s)=e^{-Ls} \tag{10}$$

$$G_2(s)=\frac{k}{s} \tag{11}$$

$$G_3(s)=\frac{1}{(1+Ts)^2} \tag{12}$$

where L is dead time, k is proportional constant and T is time constant. The transfer functions are of the linear equalized system, so proportional constant and time constant are estimated as follows. (Dead time can be directly defined.)

The indicial response $Y(s)$ of $G_2(s)\cdot G_3(s)$ is given by

$$Y(s)=\frac{k}{s^2(1+Ts)^2}\ . \tag{13}$$

Laplace inverse transformation of eq. (13) is given by

$$y(t)=k(t-2T+te^{-\frac{t}{T}}+2Te^{-\frac{t}{T}})\ . \tag{14}$$

It can be considered that $y(t)$ is corresponding to the locus of the vehicle after the onset of the steering on-off signal. Such locus can be geometrically obtained when the traveling velocity is comparatively low and the dynamic characteristics of vehicle is negligible. The lateral displacement of the vehicle Δy during time element Δt is given by

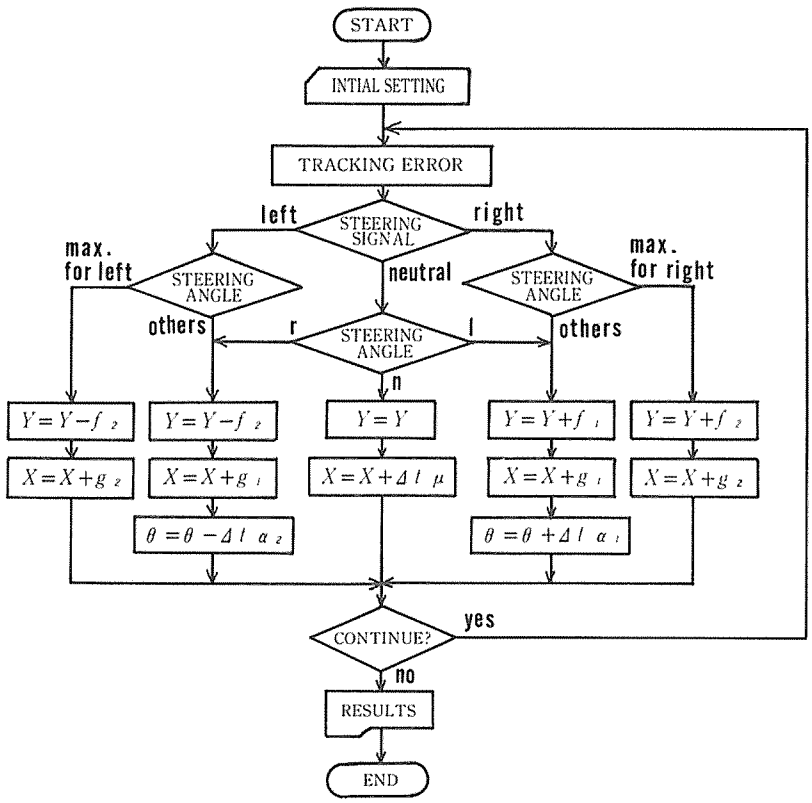

Fig. 3 Flow Chart of Digital Simulation

$$\Delta y = \Delta t v \sin\theta \tag{15}$$

where θ is steering angle and v is traveling velocity. Assuming the steering angle θ as the linear function of time, the steering angle is αt (α is a constant) at the time after the start of steering. When the steering angle is equal to the MSA, the angle is constant $\theta = \theta^*$. For the sections $0 \leqq t \leqq t^*$ and $t^* \leqq t$ (t^* is the time required to reach the MSA), the integration of eq. (15) gives

$$y_1 = -\frac{v}{\alpha}\cos\alpha t + C_1 \qquad (0 \leqq t \leqq t^*) \tag{16-a}$$

$$y_2 = v\sin\theta^* \cdot t + C_2 \qquad (t^* \leqq t) \tag{16-b}$$

in which the integration constants C_1, C_2 are

$$C_1 = \frac{v}{\alpha}$$

$$C_2 = \frac{v}{\alpha}(1 - \cos\theta^* - \theta^* \sin\theta^*) .$$

Let $t \to \infty$ in eq. (14), then

$$y(t) = k(t - 2T). \tag{17}$$

Assuming eq. (17) as eq. (16-b), proportional constant k is the inclination of the line and time constant T is the intercept on the time axis. We obtain

$$k = v\sin\theta^* \tag{18-a}$$

$$T = \frac{\theta^* \sin\theta^* + \cos\theta^* - 1}{2\alpha\sin\theta^*} \tag{18-b}$$

Digital Simulation of Control System

The flow chart of the simulation is shown in Fig. 3. In the first part, the dimensions and pattern of the desired pass, the traveling velocity and the initial position of vehicle are read. Tracking error is evaluated to decide the steering direction through three states relay with hysteresis. The vehicle position after the calculation element time Δt is calculated using the equation chosen by referring to steering angle state, as shown in the figure in which Y is the lateral position of the locus and X is the position for the direction of traveling. The lateral displacement during Δt, f_1 and f_2 are given by

$$f_1 = v\Delta t \cos\theta \tag{19-a}$$

$$f_2 = v\Delta t \cos\theta^* \tag{19-b}$$

respectively for the steering state not to reach the MSA and for the state to reach it. The displacement for the traveling direction are also given by

$$g_1 = v\Delta t \sin\theta \tag{20-a}$$

$$g_2 = v\Delta t \sin\theta^* . \tag{20-b}$$

As a hydraulic cylinder is usually used for a automated steering mechanism, the difference of the piston speed between outward and inward was reflected in the simulation program. A subprogram prepared for the dead time of control system is set up.

Results of Numerical Calculations and Simulations

In the numerical calculations and simula-

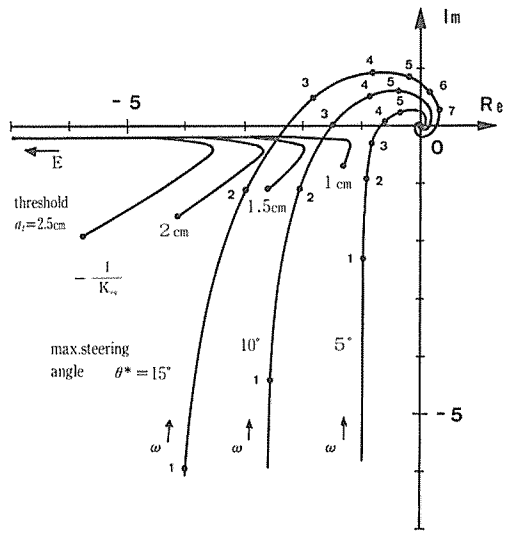

Fig. 4 Nyqist Diagram of $-1/K_{eq}$ and $G(j\omega)$

tions, parameters were taken as follows.

Traveling velocity v = 30cm/s

steering angle velocity α_1=0.699 rad/s in calculations

α_2=0.718 and 0.680 rad/s in simulations

dead time of control system L= 0.26s

hysteresis of relay $a_1 - a_2$ = 0.5cm

In the linear equalized block diagram shown in Fig. 2, the open transfer function of the linear part $G(s)$ may be found by using eq. (10), (11), (12).

$$G(s)=\frac{ke^{-Ls}}{s(1+Ts)^2} \tag{21}$$

The vector loci of $G(j\omega)$ given by eq. (21) and $-1/K_{eq}$ given by eq. (1) are shown in Fig. 4, for MSA and dead band width (DBW) as parameters. Each minimum a_1 of $-1/K_{eq}$ locus not to cross the $G(j\omega)$ locus of each MSA was calculated. With digital simulation for the step function input of 5 cm height, each minimum a_1 at stable response for each MSA from 4° to 20° was defined. The results are shown in Fig. 5 in which the curve presents the border of stability region.

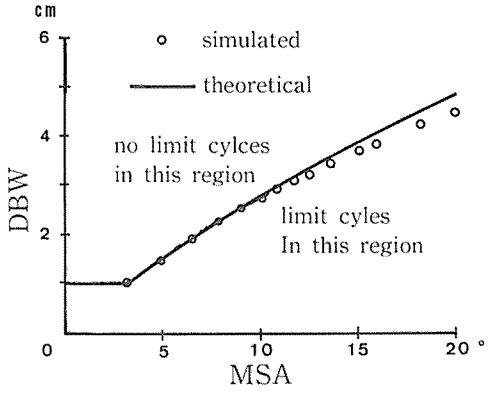

Fig. 5 Stability for Dead Band Width (DBW) vs. Maximum Steering Amgle (MSA)

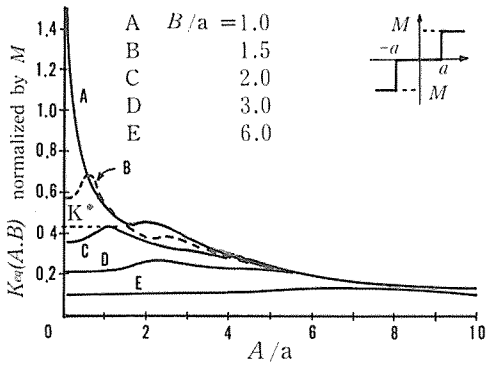

Fig. 6 Culculated Dual-input Discricing Function

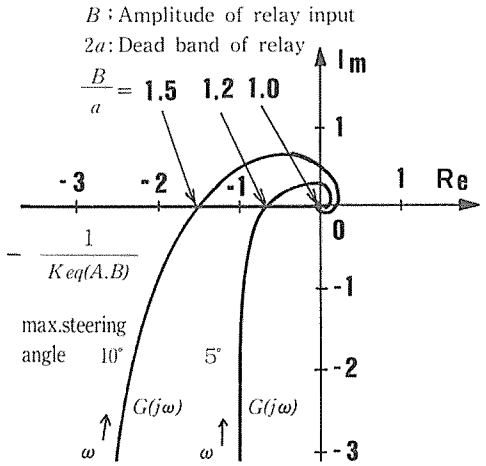

Fig. 7 Nyqist Diagram of $-1/K_{eq}$ (A, B) and $G(j\omega)$

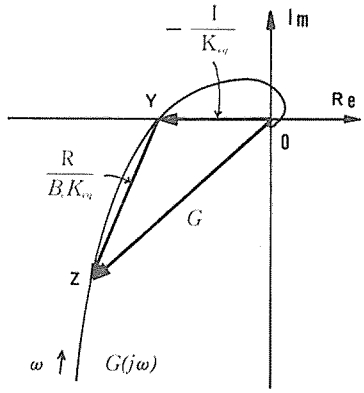

Bc: Critical input to relay

R: Critical input to system

Fig. 8 Graphical Solution of Critical Input Amplitude

Comparing theoretical and simulated results, the border of stability region was, in the simulation, estimated less lower than the theoretical in the larger steering angles. In the simulation, the steering angle velocities are not equal in out- and inward of piston and the minimum DBW for stable response is decided with the higher angle velocity. In the numerical calculations steering angle velocity can not varied in out- and inward of piston, and the velocity was assumed as the average of the both. Therefore the border of stability region was underestimated in the simulation. But the difference is small and negligible under 10° of MSA.

The responses of the system to external harmonic input were considered for the MSA 5°/ DBW 2cm and 10°/3cm which were selected from the results of above stability decision.

The plots of dual-input decribing function are shown in Fig. 6. These plots were obtained by evaluating eq. (7) and eq. (9) using digital computer. The amplitude of input signal A and $K_{eq}(A, B)$ normalized by threshold of relay a and output of relay M are respectively taken on horizontal and vertical axes. The amplitude of the other input B normalized by a are taken as parameter. Let A be the amplitude of limit cycle that may exist and B be the amplitude of input to relay. When the amplitude of input is larger than the parameter B of the curve giving the maximum value to be equal to equivalent gain (for example as shown in the figure, if $K^*=0.44$, it is curve C and $B = 2.0a$). Here B is the critical amplitude of input for the equivalent gain[13]. The Nyqist diagram of open loop transfer function $G(j\omega)$ given by eq. (21) and dual-input descricing

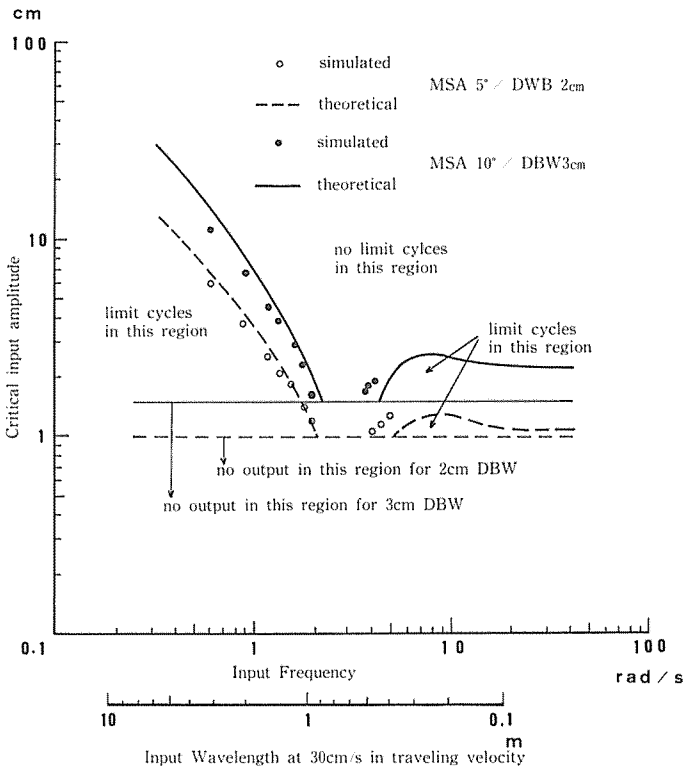

Fig. 9 Critical Input Amplitude vs. Input Frequecy

function $-1/K_{eq}(A, B)$ is shown in Fig. 7. The intercept of each vector locus of $G(j\omega)$ and $-1/K_{eq}(A, B)$ gives equivalent gain for each MSA. From each gain, we obtain each critical amplitude of input referring the plots shown in Fig. 6; the critical amplitude $B_c =$ 1.2 cm for MSA 5°(a=1cm) and B_c=2.25 cm for 10° (a=1.5cm) where the each value of a is obtained from the plots shown in Fig. 5. Each is the value at the input to relay. The value at external input may be evaluated by graphic algebra[9]. Let $R(j\omega)$ be external input, $E(j\omega)$ be input to relay, $C(j\omega)$ be output of system then

$$R(j\omega)=E(j\omega)+C(j\omega). \tag{22}$$

If E is held at B_c,

$$R=B_c+B_cK_{eq}G \tag{23}$$

where $|B_c\ K_{eq}|$ is constant. From this equation,

$$\frac{R}{B_c\,K_{eq}}=\frac{1}{K_{eq}}+G \tag{24}$$

is obtained. As shown in Fin. 8, the values of intercepts OY and YZ are graphically defined and the critical amplitude of input $|R|$ may be evaluated for each frequency by using eq. (24).

The plots of the critical amplitude of input for 5° and 10° of the MSA are shown in Fig. 9. These plots were obtained by evaluating graphically as mentioned above. The results of digital simulations are also shown in Fig. 9. These results were obtained by the simulations for each amplitude and wave length of sinusoidal desired pass. In the figure, the area over the curves or plots presents stable condition of input amplitude and frequency.

Good approximation can be seen in the frequency range under 2 rad/s, but it cannot be seen in higher range. It may be considered that the approximation of neglected hysteresis in theoretical analysis influences on the difference in high frequency region. In automatic steering system analysis, low frequency range is usually considered and the approximated method is enough useful to be applied.

Acknowledgment

The author wish to thank Prof. Noboru Kawamura, Professor Emeritus of Kyoto University, who directed author's doctor thesis "Studies on Automatic Steering and Automatic Tillage with Crab-Steering Vehicle" including this paper.

References

1) HESSE, H: *J. agric. Engng. Res.*, 19(2), 101-109, 1974
2) KAWAMURA, N *et al: J. Kansai Branch of Japanese Soc. agric. Machinery*, 46, 19-20, 1979 (in Japanese)
3) KAWAMURA, N *et al: J. Kansai Branch of Japanese Soc. agric. Machinery*, 48, 6-7, 1980 (in Japanese)
4) LOGOS, I. N.: *Grundl. Landtechnik*, 24(6), 173-176, 1974
5) UPCHURCH, B. L. *et al: Trans. ASAE*, 24(1), 29-32, 1983
6) HORIO, H. *et al: J. Japanese Soc. agric. Machinery*, 43(4), 523-531, 1982 (in Japanese with English Summary)
7) HORIO, H. *et al: J. Japanese Soc. agric. Machinery*, 44(3), 423-429, 1982 (in Japnese with English Summary)
8) HORIO, H.: *Sci. Rep. Fac. Agr. Kobe Univ.*, 16(1), 245-251, 1984 (in Japanese with English Summary)
9) GIBSON, J. E.: Nonlinear Automatic Control, McGraw-Hill, 1963
10) GIBSON, J. E., R. Sridhar: *Trans. IEEE, J. Application and Industry*, 66, 65-70, 1963
11) SRIDHAR, R., R. Oldenburger: *Trans. ASME*, 84(1), (*J. Basic Engng.*, 62), 61-67, 1962

12) WATSON, G. N.: A Treatise on the Theory of Bessel Functions, Cambridge Univ. Press, 147-148, 1922

13) OLDENBURGLR, R., R. C. Boyer: *Trans. ASME*, 84(12), (*J. Basic Engng.*, 62), 559-570, 1962

オンオフ制御によるクラブ・ステアリングの自動操向（I）
―安定解析―

堀尾尚志

要　約

クラブ・ステアリングでは、常にヨー角を変えることなくかじ取りがなされるので、車両に装着された作業機を目標経路に添わせるのが容易である。とくに平行移動的なかじ取り操作が多いほ場作業に、このかじ取り方式は利点が大きい。また、自動操向においても同様である。本報では、オンオフ制御による同かじ取り方式による自動操向システムの、調和入力に対する応答を双入力記述関数を用いて解析し、その結果をデジタル・シミュレーションの結果と比較考察した。